Adsorption of CO to Characterize the Structure of a Pd/Ag(111) Single-Atom Alloy Surface

Mark Muir and Michael Trenary*

University of Illinois at Chicago, 845 W. Taylor St. Chicago, Illinois 60607 United States

ABSTRACT: We have characterized the surface of a single-atom alloy (SAA) consisting of a low coverage of Pd deposited onto a Ag(111) surface. For this purpose, we used reflection absorption infrared spectroscopy (RAIRS) and temperature programmed desorption (TPD) of adsorbed CO. At low temperatures, a single C-O stretch band at 2047 cm^{-1} and a single CO desorption peak at 272 K were observed corresponding to CO bound to isolated palladium atoms. At palladium coverages above 0.002 ML, palladium aggregates form, as revealed by a C-O stretch peak at 1950 cm^{-1} and a desorption peak at 390 K corresponding to CO bound at the bridge sites between two palladium atoms. The diffusion of palladium from the surface into the subsurface was monitored from the C-O stretches of CO bonded to palladium and to silver atoms. Through RAIRS and TPD of CO, the ratio of surface to subsurface palladium was determined. The results from TPD experiments following H_2 exposures at low temperature indicates that dissociation of H_2 at the palladium sites does not lead to spillover of atomic hydrogen to silver atoms.

INTRODUCTION

Single-metal catalysts have been widely used in heterogenous hydrogenation reactions as they are active at modest temperatures and pressures. Expensive precious metals such as palladium, platinum, rhodium, and ruthenium can achieve high activity but often at the expense of selectivity. To achieve a better balance between activity and selectivity and to reduce cost, metal alloys have been explored by doping a catalytically active metal into a more inert metal host.[1-3] A more detailed understanding of the ligand, ensemble, and strain effects is still required to develop optimal alloy catalysts. Recently, a shift in the field of heterogenous catalysis from near-surface alloys, in which the ligand and strain effects are modified, to single-atom alloys (SAAs), in which the ensemble effects are essentially reduced to single atoms[4], has occurred. Many of these SAAs have been theoretically studied, primarily with DFT calculations, and have been predicted to break the linear scaling of the Bronsted-Evans-Polanyi (BEP) relation.[5] Although simple metal alloys can alter surface binding energies, they often follow the same linear scaling relationship of single-metal catalysts. However, with hydrogenation over a SAA, a low activation barrier to H_2 dissociation can occur on the active metal, with H atoms spilling over to the host atoms where they are weakly bound.[6] Separating the site of activation from the site of adsorption allows significant deviation from the usual linear scaling relationship. In terms of hydrogenation, the metal alloy must have a low energy barrier to dissociate molecular hydrogen, while weakly binding the atomic hydrogen, preferentially to the inert metal host. Early examples of SAAs studied experimentally include H_2 dissociation on Pt/Cu(111)[7-9] and Pd/Cu(111).[6, 10-13] These previous studies demonstrate the value of exploring the fundamental properties of new SAA combinations, with surface sensitive techniques. Infrared spectroscopy (IR) and temperature programmed desorption (TPD) of CO have been used to characterize PdCu, AuPd, and RhCu single-atom alloy surfaces.[12, 14-15] Although CO adsorption can be used to probe the surface, it can also poison or otherwise alter the catalytic activity, especially in Pt based catalyst.[16-18] In recent studies, the influence of CO on the dissociative adsorption and recombinative desorption of H_2 has been explored on the PdAu, PtCu, and PdCu single-atom alloy surfaces.[19-21]

In the present study, we use CO adsorption to characterize the Pd/Ag(111) single-atom alloy surface. The combination of Pd/Ag(111) is attractive as a SAA catalyst as it has minimal strain effects due to a lattice mismatch of only 5%. The Pd/Ag(111) interface on a Si(111) 7x7 wafer was investigated using TEM and RHEED which showed that the lattice spacing near the interface was isotropically expanded and was relaxed to the Pd bulk lattice constant at approximately 10 Pd layers, a thickness well beyond the single-atom alloy regime.[22]

Palladium deposited onto the Ag(111) surface is known to diffuse into the sub-surface of the substrate with increasing temperature. Both DFT calculations and experimental results indicate that the most stable configuration occurs through diffusion of palladium underneath a silver layer to form a capped Ag/Pd/Ag(111) surface.[23,24] $Pd_{0.8}Ag_{0.2}$(111) was modelled using DFT, and under vacuum conditions showed silver atom segregation to the surface layer with isolated surface palladium atoms being favored over palladium dimers.[23] Van Spronsen et al. observed this surface diffusion by annealing Pd/Ag(111) to 400 K and studied the surface re-arrangement induced by CO and O_2 using XPS and STM.[24]

In this study we use a combination of CO-RAIRS and CO-TPD to establish the conditions necessary to produce isolated palladium atoms on the surface with varying concentrations. The temperature at which diffusion of palladium into the subsurface region was determined from RAIRS of CO. From TPD of CO, the relative subsurface:surface palladium concentrations were determined. We also explored the ability of the surface to dissociate molecular hydrogen using TPD of H_2. Previous DFT calculations of the Pd/Ag(111) surface have shown a 0.31 eV energy barrier for H_2 dissociation and a weak binding energy of 0.33 eV for the H atoms.[25] It was concluded that spillover of

atomic hydrogen to the silver surface could occur.[25] This spill-over to the host surface is the key requirement in producing weakly bonded atomic hydrogen, possible selectivity in hydrogenation reactions, and deviation from BEP linear scaling.

EXPERIMENTAL METHODS

The experiments were performed in an ultrahigh vacuum (UHV) chamber with a base pressure of 1×10^{-10} Torr. The chamber is equipped with a PHI 10-155 cylindrical mirror analyzer for Auger electron spectroscopy (AES), PHI 15-120 optics for low energy electron diffraction (LEED), and a Hiden HAL201/3F quadrupole mass spectrometer for TPD. The UHV chamber is coupled to a Bruker IFS-66v/s Fourier-transform infrared (FTIR) spectrometer. The incident and reflected IR beams enter and exit the UHV chamber through differentially pumped, O-ring sealed KBr windows. Pressures were measured with a Bayard-Alpert hot filament ion gauge.

The silver single crystal (Surface Preparations Laboratory) is disk shaped with a diameter of 15 mm and a thickness of 2.5 mm in the (111) orientation (<0.1° accuracy). It is mounted by passing two tungsten wires through two holes (0.75 mm diameters) parallel to the (111) face in the opposite edges of the crystal. A K-type thermocouple junction is inserted into a hole in the top of the crystal (0.3 mm diameter with a depth of 0.8 mm). The crystal was cleaned with Ar sputtering (1 keV, 8 μA) and annealing to 800 K. The cleanliness of the surface was determined using LEED and AES. The lack of a RAIRS peak at 85 K for CO on Pd sites confirmed the absence of palladium below the AES detection limit.

A homemade evaporator was used to deposit Pd onto the Ag(111) surface at room temperature or at 380 K. The evaporator consists of a thin Pd wire (99.99%, Alpha Aesar) wrapped around an omega-shaped tungsten wire. RAIR spectra were obtained with 1024 scans at 4 cm^{-1} resolution. A linear heating rate of 1 K/s was used to acquire TPD results. The CO (99.99%) and hydrogen (99.999%) gases were obtained from Matheson Trigas and Praxiar, respectively. The palladium coverage was determined using AES and CO-TPD peak areas. Exposures to H_2 with the ion gauge off were based on the number of turns of the knob on the precision leak valve.

RESULTS

Figure 1 shows Auger spectra for palladium deposited onto a clean Ag(111) surface at room temperature. The Pd coverages were determined from the ratio of the peak-to-peak intensities of the MNN peak of palladium at 327 eV to the main silver peak at 351 eV and the sensitivity factors of 0.85 for palladium and 0.95 for silver.[26] The detection limit for palladium by AES was approximately 0.015 ML, and coverages below this limit were determined from CO TPD peak areas. As there are a number of assumptions involved in determining accurate absolute Pd coverages from AES, we used AES mainly to provide a precise way to measure the relative Pd coverages and to vary them in a systematic way.

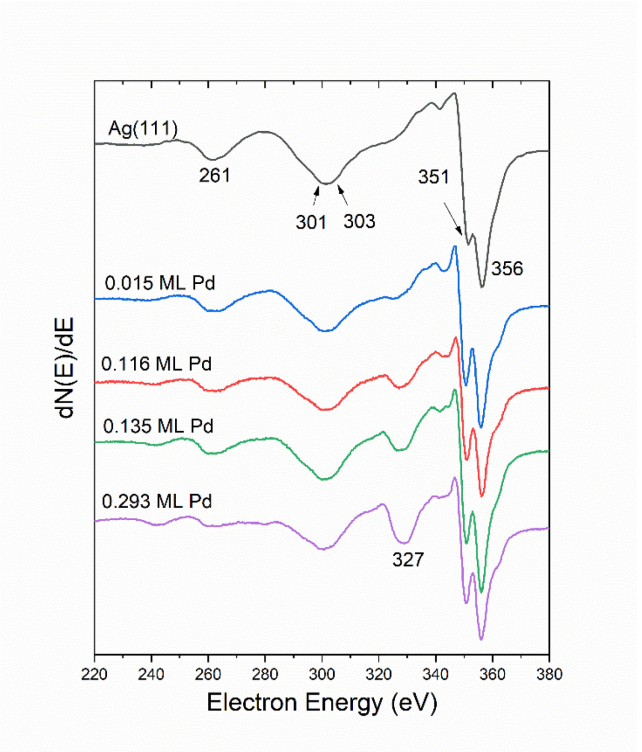

Figure 1. Auger spectra of Ag(111) and Pd/Ag(111) for increasing palladium coverage.

CO was used to probe the Pd/Ag(111) surface as CO chemisorbs on palladium but only weakly physisorbs on silver. Figure 2 shows a series of RAIR spectra obtained by exposing 1 L of CO to Ag(111) at 85 K with the indicated coverages of palladium. A 1 L (1 L (Langmuir) = 1×10^{-6} Torr sec) exposure was found to saturate the surface as no changes were observed with additional CO doses. The physisorption of CO on Ag(111) has been extensively studied using HREELS, ARUPS, STM, and TDS.[27] As shown in Figure 2, a saturation coverage of CO on clean Ag(111) gives rise to a single weak ν(CO) peak at 2147 cm^{-1}. Hansen et. al. observed this peak with HREELS at 265 meV (2137 cm^{-1}) for coverages from sub-monolayer to multilayers at 35 K. This is near the value for gas phase CO at 266 meV (2145 cm^{-1}), indicating that CO is physisorbed on Ag(111).[27] We therefore assign the peak at 2148 cm^{-1} to CO on Ag(111).

At 0.001 ML Pd/Ag(111), a ν(CO) stretch was observed at 2047 cm^{-1} corresponding to CO adsorbed at on-top sites of palladium atoms. By increasing the palladium coverage to 0.010 ML, a second ν(CO) stretch was observed at 1950 cm^{-1} corresponding to CO adsorbed at bridge sites between palladium atoms, indicating palladium dimer formation. The upward IR peak at 1817 cm^{-1} is due to background CO adsorbed at three-fold hollow sites of two-dimensional Pd clusters.[14] This peak was present during the background scans of the nominally clean surface. Upon deliberate exposure to CO, the adsorbed CO shifts to Pd two-fold bridge sites with C-O stretch values of 1950-1958 cm^{-1}, causing the 1817 cm^{-1} peak to appear in the upward direction in the ratio spectra.

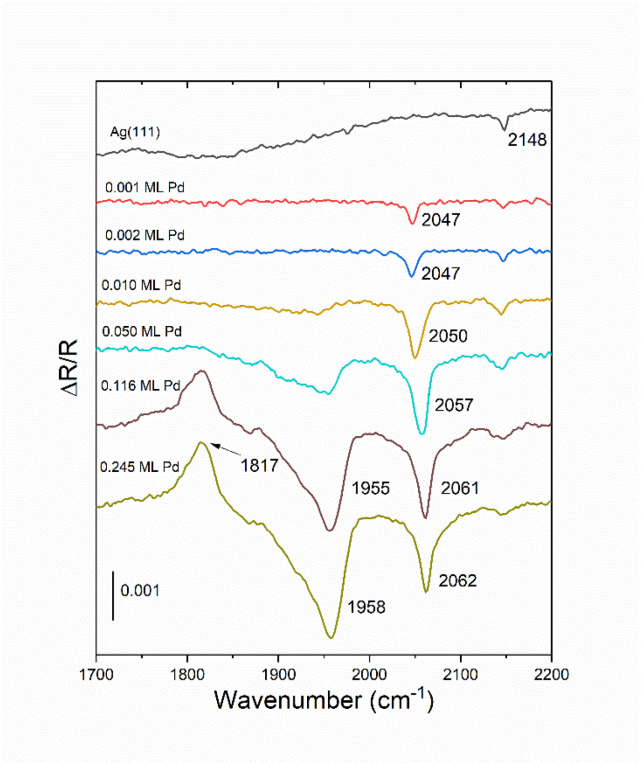

Figure 2. RAIR spectra taken at 85 K of CO at saturation coverage on Ag(111) and Pd/Ag(111) at various palladium coverages. Pd was deposited on Ag(111) at room temperature.

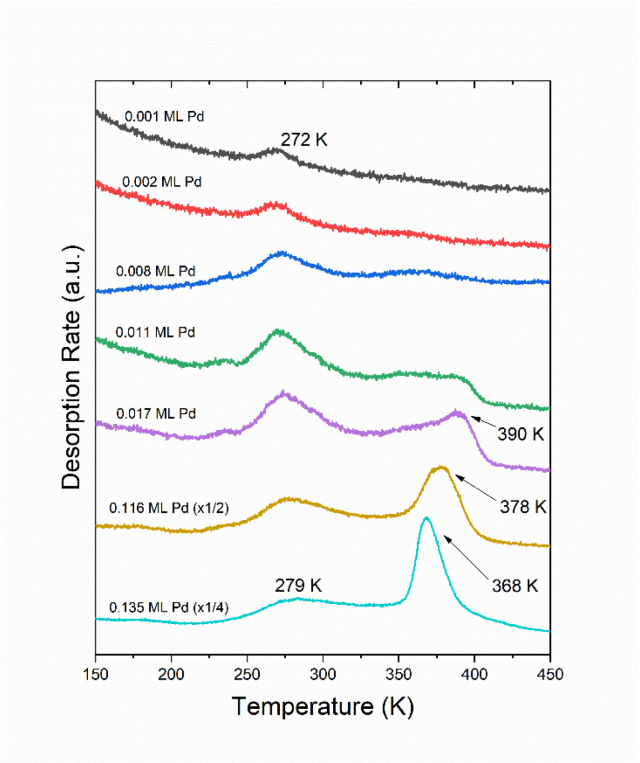

Figure 3. TPD spectra of CO at saturation coverage on Pd/Ag(111) at various palladium coverages taken from 95 K to 450 K. A linear heating rate of 1 K/s was used. Pd was deposited onto Ag(111) at room temperature.

The broad asymmetric C-O stretch peak seen in Figure 2 at 1958 cm^{-1} has a similar appearance to the peak at 1954 cm^{-1} reported by Manzi et al.[14] for $^{12}C^{16}O$ on Pd(111) at a coverage of 0.66 ML at 90 K. In their work, they showed by using $^{12}C^{16}O$ and $^{13}C^{16}O$ mixtures that the peak shifts to higher wavenumber due to dipole-dipole coupling between CO molecules. This then implies that the peak that we observe in Figure 2 corresponds to multiple CO molecules on aggregates of Pd, rather than to isolated Pd dimers, where dipole-dipole coupling shifts would not occur.

Figure 3 shows CO TPD results after the Pd/Ag(111) surfaces were cooled to 85 K, dosed with CO, and annealed to 95 K (to desorb CO from Ag sites) before starting the TPD ramps. For the 0.001 ML and 0.002 ML Pd/Ag(111) surfaces (black and red traces), a single desorption peak is observed at 272 K corresponding to CO desorption from the on-top sites of palladium atoms. At higher palladium coverage, a second desorption peak is observed at 390 K corresponding to CO desorption from Pd bridge sites.[28] From the TPD spectra, we can see that palladium aggregation begins to dominate around 0.02 ML Pd.

Figure 4 compares results for low coverages of Pd following Pd deposition at room temperature and at 380 K. We show that for room temperature deposition, the onset for Pd aggregation occurs at 0.0028 ML (green). However, at a deposition temperature of 380 K, Pd aggregation has not occurred at 0.0029 ML (gold).

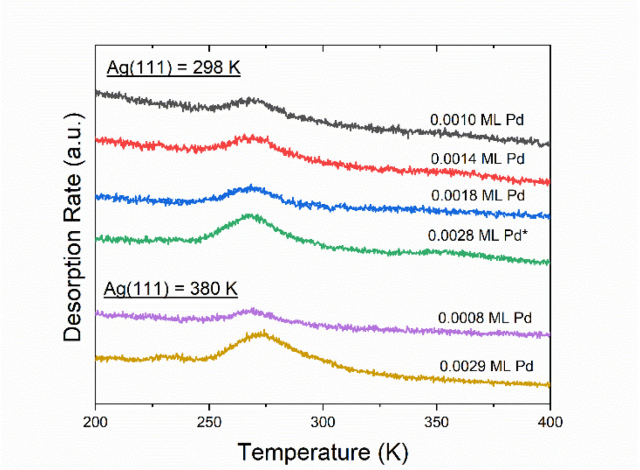

Figure 4. A comparison of CO TPD spectra for Pd/Ag(111) in the single-atom alloy regime. The Ag(111) temperatures denote the crystal temperature during palladium deposition. The asterisk indicates the beginning of palladium aggregation, as revealed by CO desorption at 360 K.

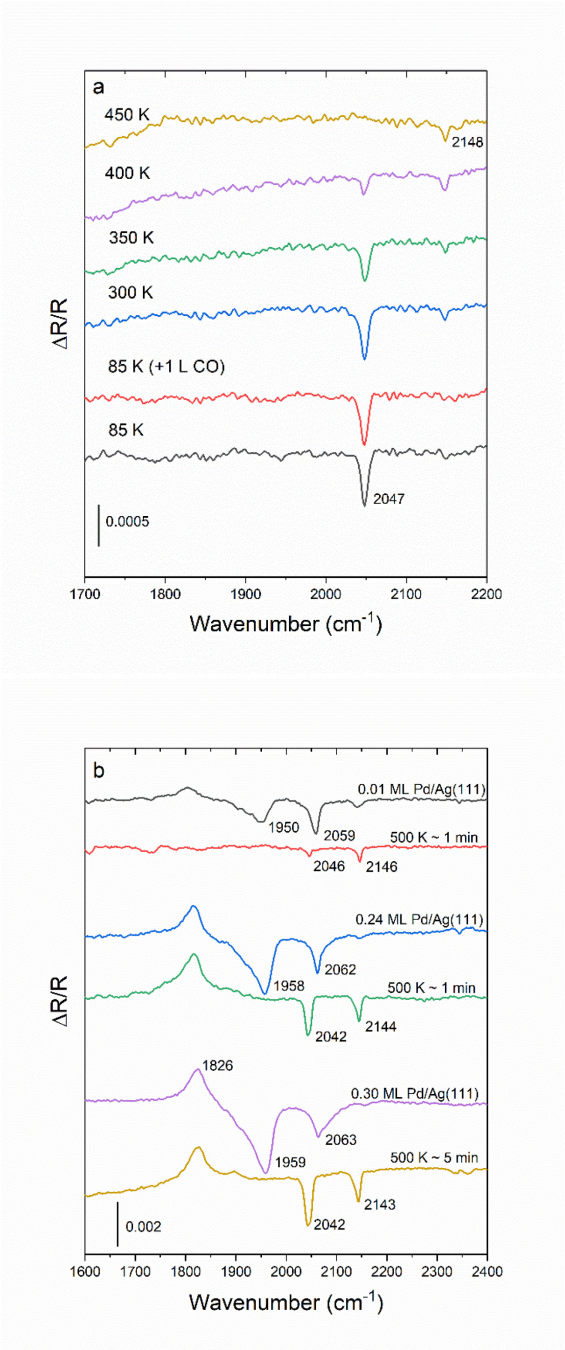

Figure 5. (a) RAIRS spectra of CO at saturation coverage on 0.001 ML Pd/Ag(111) at 85 K (black) and exposed to an additional 1 L of CO (red). Each subsequent spectrum was annealed to the indicated temperature for one minute, re-cooled, and exposed to an additional 1 L of CO. (b) RAIRS spectra of various Pd/Ag(111) coverages dosed with CO at 85 K, annealed to 500 K, re-cooled, and exposed to an additional 1 L of CO.

The stability versus temperature of the Pd/Ag(111) SAA surface was studied using RAIRS and TPD of CO. Figure 5a shows RAIR spectra of 0.001 ML Pd/Ag(111) initially dosed with 1 L of CO at 85 K. By dosing an additional 1 L of CO, no change was seen in the RAIR spectra, indicating saturation of the surface. Upon annealing to the indicated temperatures for one minute, re-cooling the crystal, and re-dosing with CO, the intensity of the CO-Pd (on-top) IR band decreases and completely disappears by 450 K. This indicated that palladium had diffused into the subsurface. As the CO-Pd peak disappears, an IR band at 2148 cm^{-1} reappears due to CO on Ag.

By annealing higher palladium coverages to 500 K, the results in Figure 5b show that the IR band at 2042 cm^{-1} (CO at Pd on-top sites) is larger (green, gold) than it was prior to annealing (blue, violet). We also see a complete loss of the 1950 cm^{-1} peak (CO at Pd bridge sites) and from the decrease in the total IR peak area, we conclude that there is a net loss in exposed Pd atoms on the surface. The 500 K anneal also enhances the peak at 2146-2143 cm^{-1} due to CO on Ag. As described more fully in the discussion section, these results are consistent with Ag atoms covering Pd islands, hence eliminating Pd dimer sites, while leaving some isolated Pd atoms on the Ag(111) surface. From the RAIRS results alone, it is difficult to distinguish Pd diffusion into the subsurface region versus Ag atom migration to cap Pd islands. It is likely that both processes occur simultaneously.

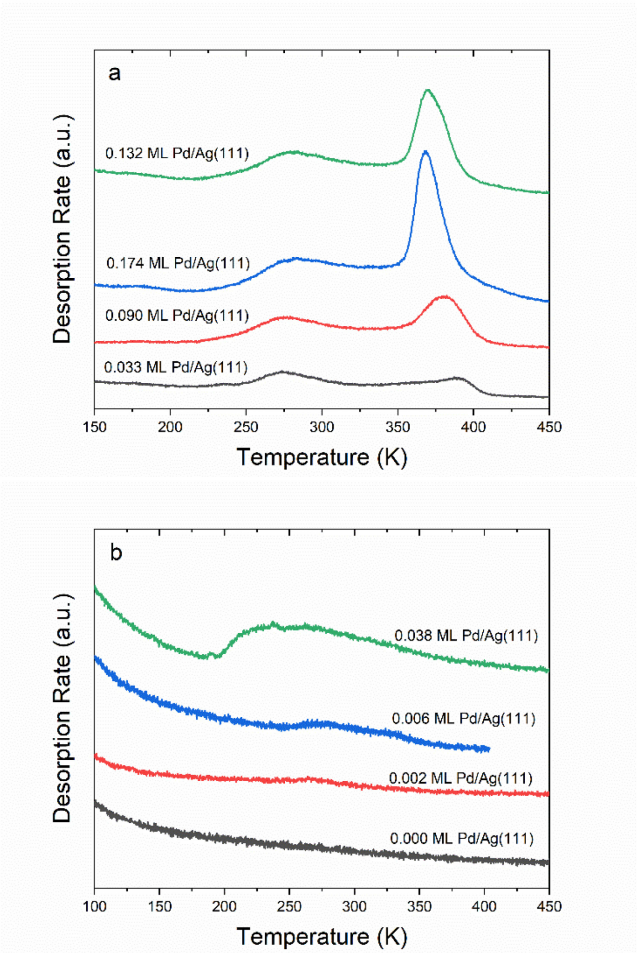

Figure 6. (a) CO-TPD spectra of 0.33, 0.090, 0.132, and 0.174 ML Pd/Ag(111). The crystal was heated at a linear rate of 1 K/s from 95 to 500 K and held at 500 K for 30 seconds (green) or one minute (black, red, blue). (b) Following re-cooling of the surface, a second set of CO-TPD spectra were taken up to 450 K. The Pd coverages for the second set of TPD results are based on CO TPD peak areas.

The diffusion of palladium into the silver subsurface region was also studied using CO-TPD to quantify the increased coverage

of isolated Pd atoms. The CO TPD results in Figure 6b were obtained for four coverages of Pd. After exposure to 1 L of CO, the surface was linearly ramped to 500 K, and then held at 500 K for one minute (Figure 6a). Leaving the surface at 500 K for one minute caused the palladium to diffuse into the subsurface. Exposure to additional CO allows palladium remaining on the surface to be detected with TPD. After annealing the 0.033 ML Pd/Ag(111) surface, a flat TPD spectrum (Figure 6b, black) was obtained. This indicates that all the palladium diffused into the subsurface so this trace is labelled as 0.000 ML Pd/Ag(111). For initial Pd coverages of 0.090 ML and 0.174 ML, however, some palladium remained on the surface following annealing. Using CO-TPD peak areas, the remaining surface palladium coverages were determined to be 0.002 ML and 0.006 ML, respectively. By subtracting the palladium coverages in Figure 6b from those in Figure 6a, the subsurface palladium coverages could also be determined (0.088 ML and 0.168 ML, respectively). The green spectrum in Figure 6a was obtained after annealing to 500 K for only 30 seconds, and gave rise to a larger Pd-SAA coverage in 6b due to the shorter time for diffusion. Further annealing of the Pd/Ag(111) surface above 700 K leads to palladium diffusion into the bulk as indicated by the loss of the Pd Auger MNN peak at 327 eV.

In Figure 7, we show H_2 TPD following a 50 L exposure of molecular hydrogen to the clean Ag(111) surface at 85 K with and without the ion gauge on. The hot cathode ionization gauge dissociates some of the molecular hydrogen into H atoms providing a way to adsorb atomic hydrogen on the surface.

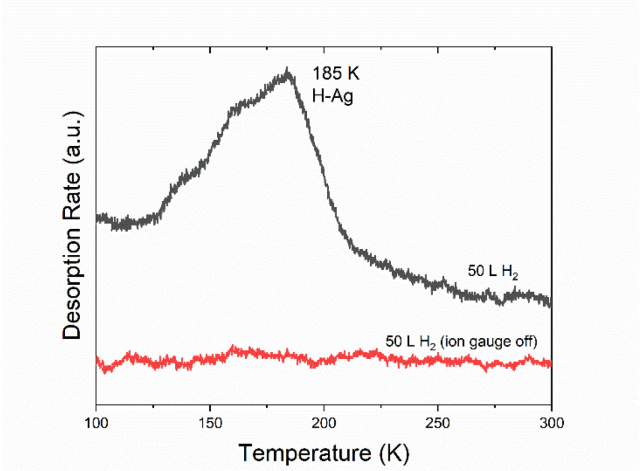

Figure 7. TPD spectra from 95 K to 300 K following a 50 L H_2 exposure to Ag(111) at 85 K taken with the ion gauge on (black) and off (red).

When the ion gauge was turned off during exposure, no H_2 desorption is seen, indicating that hydrogen is not activated on silver, as expected. However, with the ion gauge on, a desorption peak is seen at 185 K (Figure 7, black). Previous studies are in agreement that hydrogen desorbs at 185 K from Ag(111) when exposed to atomic hydrogen.[29-30] Figure 8 shows H_2 TPD results for increasing hydrogen exposures to a 0.008 ML Pd/Ag(111) SAA surface with and without the ion gauge on. The SAA surface shows two desorption peaks at 147 and 180 K (Figure 8a) for a 10 L H_2 exposure with the ion gauge on. These peaks shift to 137 and 177 K for a 50 L H_2 exposure. The lower temperature desorption peak is not seen in Figure 6 on Ag(111), and therefore is attributed to recombinitive desorption at palladium atoms. The higher temperature desorption peaks correspond to recombinative desorption of hydrogen from silver sites. By increasing the palladium coverage, the H_2-TPD spectra show exclusive desorption at the lower temperature, which has a peak at 148 K for a 200 L H_2 exposure. We interpret this as the Pd atoms providing a lower temperature pathway for recombinative desorption of the H atoms that adsorbed on the Ag(111) sites through exposure to H atoms. Essentially all the hydrogen can desorb through the lower temperature pathway for the higher Pd coverage used for the results in Figure 8b than in Figure 8a.

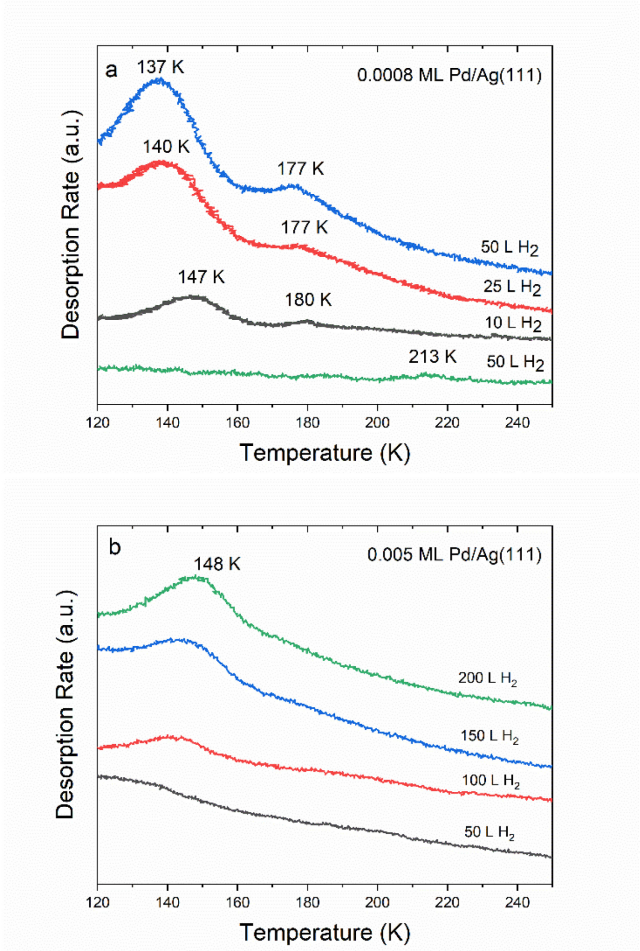

Figure 8. (a) H_2 TPD spectra on 0.0008 ML Pd/Ag(111) with increasing hydrogen coverage with the ion gauge on (black, red, and blue) and 50 L H_2 taken with the ion gauge off (green). (b) H_2 TPD spectra on 0.005 ML Pd/Ag(111) with increasing hydrogen coverage with the ion gauge on.

DISCUSSION

The results presented here using RAIRS and TPD of CO to probe Pd/Ag(111) imply that at sufficiently low Pd coverages, isolated Pd atoms exist in the topmost atomic layer of the Ag(111) surface. We therefore concluded that under the right conditions, Pd/Ag(111) can form a SAA. This conclusion needs to be reconciled with other studies of the Pd/Ag(111) surface, including recent work indicating that the adsorption of CO can stabilize surface Pd, thus possibly invalidating the use of CO to probe the structure of Pd/Ag(111). In many ways, conclusions from some of these studies are not necessarily applicable to our

results because of differences in Pd coverage, preparation temperatures, or CO pressures. Nevertheless, the fact that the different studies explored different ranges of parameters leads to a more complete understanding of the Pd/Ag(111) system.

Darby et al.[4] carried out extensive theoretical studies on a series of SAA alloys, including Pd/Ag(111). They used DFT to determine the energetics of various Pt-group metal dopants on the (111) surfaces of Cu, Ag, and Au. They find that ΔE_{seg}, the energy change for a single Pd atom to migrate from the surface to the bulk, is -0.21 eV. This is consistent with our inference that Pd diffuses into the Ag bulk after annealing the surface to 450 K. The DFT calculations of Darby et al.[4] were done for a 3×3×5 slab, so a single surface Pd atom corresponds to a Pd coverage of 0.11 ML, which is considerably higher than the lowest coverages that we investigated. While low coverages of 1% or less are not difficult to study experimentally, they require very large unit cells in DFT studies, which demand considerable computational resources. Van Spronsen et al.[24] also employed DFT as part of a combined computational and experimental study of the Pd/Ag(111) surface. They used both 3×3×6 and 2×2×6 slab models, again placing a lower limit on the Pd coverage of 0.11 ML. They also found that the subsurface alloy was more stable than the surface alloy (the SAA). Both alloys are considerably more stable than structures with Pd atoms on top of the surface. Darby et al.[4] also calculated the energy associated with aggregation of dopant atoms relative to the SAA phase. The calculated energies of formation of various Pd aggregates were all positive relative to the SAA phase, indicating that the latter should be stable with respect to aggregation into Pd islands in the topmost surface layer.

Van Spronsen et al.[24] also reported experimental STM images of 0.2 ML of Pd deposited onto Ag(111) at room temperature and after annealing to 405 K. For room temperature deposition, fractal-shaped Pd islands one-Pd-layer high were observed along with some monolayer vacancies and some Ag-capped Pd islands. Annealing to 405 K produced mainly Ag-capped Pd islands, adjacent to monolayer pits in the Ag surface. The results in our Figure 5 can be explained in light of these STM observations. We found that for the annealed surface with an initial Pd coverage of 0.24 ML, CO adsorbs only on Pd top sites, as indicated by a peak at 2042 cm^{-1} and on Ag atoms, as indicated by the peak at 2144 cm^{-1}. Peaks due to CO adsorption at Pd bridge-sites are eliminated by the annealing, indicating that intermingling of Ag and Pd atoms in the islands has eliminated structures with adjacent Pd atoms. As the 2144 cm^{-1} peak is at essentially the same value as the 2148 cm^{-1} peak observed in Figure 2 on the bare Ag(111) surface, where it was attributed to step site adsorption, the 2144 cm^{-1} peak in Figure 5b, can be assigned to CO adsorbed on Ag atoms at the edges of Ag-capped Pd islands. The greater abundance of these edge sites for a surface with many such islands would account for the enhanced intensity of the 2146-2143 cm^{-1} peak in Figure 5. Although the STM results of Van Spronsen et al.[24] do not show the presence of the isolated Pd atoms implied by the C-O stretch peak at 2042 cm^{-1}, the exposed but isolated Pd atoms may either be in the Ag-capped Pd islands or elsewhere on the Ag(111) surface. Our results indicate that even for high Pd coverages, annealing the surface still leaves some isolated Pd atoms available for CO adsorption. Figure 9 provides a structural model consistent both with Ag-capped Pd islands and our results.

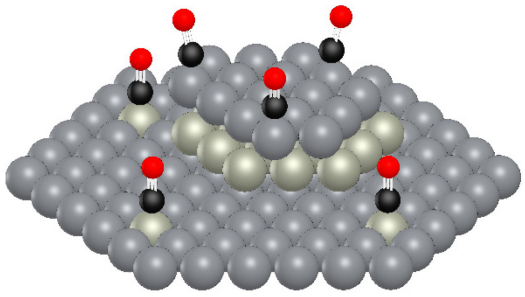

Figure 9. Illustration of a Ag(111) surface with a Ag-capped-Pd island consistent with the annealing results shown in Figure 5b.

Darby et al.[31] also calculated the adsorption energies and vibrational frequencies of CO adsorbed on the host metals and SAAs. For CO adsorbed on Ag(111), they calculated a C-O stretch of 2015 cm^{-1} for CO bound at atop sites, the most stable sites for this surface. This compares to our observed value of 2143-2148 cm^{-1}. For CO bound on top of a Pd atom in the Pd/Ag(111) SAA surface, they calculate a C-O stretch frequency of 1982 cm^{-1}, compared to our measured values in the range of 2042-2067 cm^{-1}. The 3 to 4% difference between the calculated and experimental frequencies for CO on Pd/Ag(111) is within the typical error for such calculations. The bigger difference for CO on Ag(111) may be because the calculated value is for CO at a terrace site, whereas the experimental value is likely due to CO at Ag step sites. It is known, for example, that CO is more strongly bound at the step sites of Pt(111) than at the terrace sites, and that the C-O stretch frequencies are different at the two sites[32]. Darby et al.[31] used transition state theory and kinetic Monte Carlo (kMC) simulations to predict CO TPD results for direct comparison to experimental results such as ours. The peak of the CO TPD trace was calculated to be at about 300 K for Pd/Ag(111), which is about 200 K lower than the calculated peak at about 500 K for CO on Pd(111). The latter is compared to experimental CO TPD results of Guo et al.[28], who found that CO desorbs from Pd(111) as a narrow peak at about 500 K at the lowest CO coverages. However, the CO desorbs over a broader range that extends to as low as 200 K at the highest coverages. In our Figure 6a, we see CO desorption from the Pd/Ag(111) SAA in the range of 270-280 K, but from the Pd(111) islands at 370-390 K. The experimental results of Guo et al.[28] indicate that lateral interactions significantly lower the CO desorption temperature, whereas such interactions are not included in the calculations of Darby et al.[31] We therefore interpret the lower temperatures for CO desorption that we observe from both the Pd/Ag(111) SAA and from the Pd islands as due to lateral interactions that are not included in the calculations.

Both Darby et al.[31] and van Spronsen et al.[24] considered the influence of CO on the structure and stability of Pd/Ag(111). Darby et al.[31] concluded that CO adsorption would favor aggregation of Pd on Ag(111), allowing the CO to thereby adsorb on Pd bridge sites. As we clearly detect CO adsorption at Pd top sites, without any bridge site CO, for low Pd coverages, there

must be a kinetic barrier preventing aggregation. The presence of the kinetic barrier to CO-induced aggregation indicates that CO can probe the structure that the Pd/Ag(111) surface has prior to CO adsorption. Van Spronsen et al.[24] also considered the influence of CO on the stability of surface versus subsurface Pd in both their calculations and ambient pressure XPS experiments. They concluded that in the presence of an ambient pressure of CO, Pd is drawn from the subsurface to the surface region. Once drawn to the surface by the CO, the Pd remains stable on the surface as the CO pressure is reduced. However, under the low CO pressure conditions that we have used, we find that once Pd has diffused into the subsurface region, CO adsorption does not induce the Pd to diffuse back to the surface. For example, in Figure 5a, after the surface had been annealed to 450 K and re-exposed to CO, the C-O stretch peak due to CO on Pd does not reappear. Thus, under the conditions we have used here, the CO acts as a passive probe of the structure of the Pd/Ag(111) surface.

Our hydrogen TPD results can be compared and contrasted with results reported by Lucci et al.[19] for a Pd/Au(111) SAA. Using STM, they showed that at Pd coverages below 0.05 ML, an SAA forms with isolated Pd atoms substituting for Au atoms in the topmost layer. They found that H_2 dissociated on the Pd/Au(111) SAA surface at 85 K and led to a main H_2 TPD peak at 175-200 K, and a minor peak at 110 K. They attributed the higher temperature peak to recombinative H_2 desorption at the Pd sites, with the lower temperature peak due to desorption from Au sites. Coadsorbed CO blocked the Pd sites for H_2 desorption and led to spillover of H atoms to the Au sites, thus enhancing the H_2 desorption at 110 K relative to the higher temperature desorption channel. The conclusion that the 175-200 K H_2 desorption occurred at the Pd atoms was supported by the linear increase of the area of this peak with Pd coverage. The experimental observation of a low temperature H_2 desorption peak contrasted with the results from DFT calculations that showed a barrier for H_2 desorption from Au sites of 1.04 eV, but only 0.20 eV from the Pd/Au(111) sites. In our case, we are unable to detect H_2 dissociation on the Pd/Ag(111) surface. This is likely due to the much lower Pd coverages needed to achieve the SAA structure for Pd/Ag(111). It seems likely that H_2 would dissociate on Pd sites of the Pd/Ag(111) SAA, but if no H atom spillover occurs, then H atom adsorption would be confined to the Pd sites, which are too few in number to give rise to a detectable H_2 desorption peak. When we populated the Ag(111) surface with H atoms through H atom exposure via the ion gauge, we observe an H_2 desorption channel that peaks at 185 K. A lower temperature H_2 channel in the range of 137-148 K is observed in the presence of Pd atoms. These results imply a higher barrier for H_2 desorption from the host sites than from the Pd sites, as predicted in the DFT calculations of Lucci et al.[19] They speculated that the low temperature pathway for H_2 desorption from Au(111) may have involved quantum mechanical tunneling. Presumably, this pathway is not available on Ag(111), and the temperatures for desorption from the Pd and Ag sites follows the presumed order of the activation barriers for desorption.

Our conclusion that in contrast to Pd/Cu(111), H atom spillover does not occur on the Pd/Ag(111) SAA can be rationalized by the relative energetics. The adsorption energies of H on the energetically favored fcc hollows sites of Cu(111), Au(111), and Ag(111) have been calculated by Greeley and Mavrikakis as -2.38, -2.22, and -2.08 eV, respectively.[33] Tierney et al. reported DFT calculations of H spillover on Pd/Cu(111) and Pd/Au(111).[34] They calculated ΔG values for the spillover and concluded that while spillover was thermodynamically favored for Pd/Cu(111), it was not for Pd/Au(111). The lack of H atom spillover on the Pd/Au(111) SAA was confirmed in the STM work of Barber et al.[35] As the binding energy of the H atom is similar at a site with one Pd atom and two Cu atoms or one Pd atom and two Au atoms, the difference in the thermodynamics of spillover in the two cases lies mainly in the lower binding energy at the Au(111) sites. The weaker binding energy of H on Ag(111) than on Au(111), would then imply that if spillover doesn't occur for Pd/Au(111), it wouldn't occur on Pd/Ag(111) either. However, based on their calculations of the Pd/Ag(111) surface, Aich et al. concluded that H atom spillover could occur on this surface.[25] This illustrates the importance of independent experimental investigation of the spillover effect.

CONCLUSION

At Pd coverages up to approximately 0.002 ML, we find that Pd/Ag(111) forms a single-atom alloy. The observation of CO adsorption at Pd atop sites but not at Pd bridge sites indicates that the Pd atoms are isolated from each other. The SAA structure is not stable with respect to a subsurface alloy, or diffusion of Pd into the bulk, as indicated by the disappearance of isolated Pd atom sites upon annealing the surface to 450 K. This is consistent with formation of Ag-capped Pd islands, as reported by others. Exposure of the Pd/Ag(111) to H_2 does not lead to a measurable amount of H_2 desorption. As studies of similar SAAs have found H_2 dissociation at isolated Pd atoms, we assume that H_2 also dissociates at the Pd sites of the Pd/Ag(111) surface, but that no spillover of H atoms to Ag sites occurs. This explains why there was insufficient H atom coverage to produce a measurable H_2 desorption peak. By exposure of the surface to atomic H, we find that H_2 desorbs from Pd sites with a lower activation barrier than desorption from Ag sites.

AUTHOR INFORMATION

Corresponding Author

* E-mail: mtrenary@uic.edi

ACKNOWLEDGMENT

This work was supported by a grant from the National Science Foundation, CHE-1800236. We thank Professor E. C. H. Sykes for insightful discussions and for sharing unpublished STM results with us. We thank Mr. Arephin Islam for assistance with the manuscript preparation.

REFERENCES

(1) Rodriguez, J. A.; Physical and Chemical Properties of Bimetallic Surfaces. *Surf. Sci. Rep.* **1996**, 24, 223-287.

(2) Greenley, J.; Mavrikakis, M. Alloy Catalysts Designed From First Principles. *Nat. Mater.* **2004**, 3, 810-815.

(3) Chen, J. G.; Menning, C. A.; Zellner, M. B. Monolayer Bimetallic Surfaces: Experimental and Theoretical Studies of Trends in Electronic and Chemical Properties. *Surf. Sci. Rep.* **2008**, 63, 201-254.

(4) Darby, M. T.; Stamatakis, M.; Michaelides, A.; Sykes, E. C. H. Lonely Atoms with Special Gifts: Breaking Linear Scaling Relationships in Heterogeneous Catalysis

with Single-Atom Alloys. *J. Phys. Chem. Lett.* **2018**, 9, 5636-5646.

(5) Darby, M. T.; Réocreux, R.; Sykes, E. C. H.; Michaelides, A.; Stamatakis, M. Elucidating the Stability and Reactivity of Surface Intermediates on Single-Atom Alloy Catalysts. *ACS Catal.* **2018**, 8, 5038-5050.

(6) Kyriakou, G.; Boucher, M. B.; Jewell, A. D.; Lewis, E. A.; Lawton, T. J.; Baber, A. E.; Tierney, H. L.; Flytzani-Stephanopoulos, M.; Sykes, E. C. H.; Isolated Metal Atom Geometries as a Strategy for Selective Heterogenous Hydrogenations. *Science* **2012**, 335, 1209-1212.

(7) Lucci, F. R.; Lawton, T. J.; Pronschinske, A.; Sykes, E. C. H.; Atomic Scale Surface Structure of Pt/Cu(111) Surface Alloys *J. Phys. Chem. C* **2014**, 118, 3015-3022.

(8) Lucci, F. R.; Liu, J.; Marcinkowski, M. D.; Yang, M.; Allard L. F.; Flytzani-Stephanopoulos, M.; Sykes, E. C. H.; Selective Hydrogenation of 1,3-butadiene on Platinum-Copper Alloys at the Single-Atom Limit. *Nat. Commun.* **2015**, 6, 8550.

(9) Lucci, F. R.; Marcinkowski, M. D.; Lawton, T. J.; Sykes, E. C. H.; H_2 Activation and Spillover on Catalytically Relevant Pt-Cu Single Atom Alloys. *J. Phys. Chem. C* **2015**, 119, 24351-24357**.**

(10) Cao, X. X.; Mirjalili, A.; Xie, W. T.; Jang, B. W. L. Investigation of the Preparation Methodologies of Pd-Cu Single-Atom Alloy Catalysts for Selective Hydrogenation of Acetylene. *Front. Chem. Sci. Eng.* **2015**, 9, 442-449.

(11) Pei, G. X.; Liu, X. Y.; Yang, X.; Zhang, L.; Wang, A.; Li, L.; Wang, H.; Wang, X.; Zhang, T. Performance of Cu-Alloyed Pd Single-Atom Catalyst for Semihydrogenation of Acetylene under Simulated Front-End Conditions. *ACS Catal.* **2017**, 7, 1491-1500.

(12) Kruppe, C. M.; Krooswyk, J. D.; Trenary, M. Polarization-Dependent Infrared Spectroscopy of Adsorbed Carbon Monoxide to Probe the Surface of a Pd/Cu(111) Single-Atom Alloy. *J. Phys. Chem. C* **2017**, 121, 9361-9369.

(13) Kruppe, C. M.; Krooswyk, J. D.; Trenary, M. Selective Hydrogenation of Acetylene to Ethylene in the Presence of a Carbonaceous Surface Layer on a Pd/Cu(111) Single-Atom Alloy. *ACS Catal.* **2017**, 7, 8042-8049.

(14) Manzi, S.; Brites Helú, M. A.; Tysoe, W. T.; Calaza, F. C. Combining IR Spectroscopy and Monte Carlo Simulations to Identify CO Adsorption Sites on Bimetallic Alloys. *J. Phys. Chem. C* **2019**, 123, 8406-8420.

(15) Hannagan, R. T.; Patel, D. A.; Cramer, L. A.; Schilling, A. C.; Ryan, P. T. P.; Larson, A. M.; Çınar, V.; Wang, Y.; Balema, T. A.; Sykes, E. C. H. Combining STM, RAIRS and TPD to Decipher the Dispersion and Interactions Between Active Sites in RhCu Single-Atom Alloys. *ChemCatChem* **2019**, 11, 1-7.

(16) Cheng, X.; Shi, Z.; Glass, N.; Zhang, L.; Zhang, J.; Song, D.; Liu, Z. S.; Wang, H.; Shen J. A Review of PEM Hydrogen Fuel Cell Contamination: Impacts, Mechanisms, and Mitigation. *J. Power Sources* **2007**, 165, 739-756.

(17) Baschuk, J. J.; Li, X. Carbon Monoxide Poisoning of Proton Exchange Membrane Fuel Cells. *Int. J. Energy Res.* **2001**, 25, 695-713.

(18) Liu, J.; Lucci, F. R.; Yang, M.; Lee, S.; Marcinkowski, M. D.; Therrien, A. J.; Williams, C. T.; Sykes, E. C. H. Tackling CO Poisoning with Single-Atom Alloy Catalysts. *J. Am. Chem. Soc.* **2016**, 138, 6396-6399.

(19) Lucci, F. R.; Darby, M. T.; Mattera, M. F. G.; Ivimey, C. J.; Therrien, A. J.; Michaelides, A.; Stamatakis, M.; Sykes, E. C. H. Controlling Hydrogen Activation, Spillover, and Desorption with Pd-Au Single-Atom Alloys. *J. Phys. Chem. Lett.* **2016**, 7, 480-485.

(20) Darby, M. T.; Lucci, F. R.; Marcinkowski, M. D.; Therrien, A. J.; Michaelides, A.; Stamatakis, M.; Sykes, E. C. H. Carbon Monoxide Mediated Hydrogen Release from PtCu Single-Atom Alloys: The Punctured Molecular Cork Effect. *J. Phys. Chem. C* **2019**, 123, 10419-10428.

(21) Marcinkowski, M. D.; Jewell, A. D.; Stamatakis, M.; Boucher, M. B.; Lewis, E. A.; Murphy, C. J.; Kyriakou, G.; Sykes, E. C. H.; Controlling a Spillover Pathway with the Molecular Cork Effect. *Nat. Mat.* **2013**, 12, 523-528.

(22) Aoki, Y. Lattice Spacing Distribution at Pd/Ag(111) Interface by Transmission Electron Microscopy. *Phys. Astron. Int. J.* **2018**, 2, 213-216.

(23) Gonzalez, S.; Neyman, K. M.; Shaikhutdinov, S.; Freund, H.; Illas, F. On the Promoting Role of Ag in Selective Hydrogenation Reactions over Pd-Ag Bimetallic Catalysts: A Theoretical Study. *J. Phys. Chem. C* **2007**, 111, 6852-6856.

(24) Van Spronsen, M. A.; Daunmu, K.; O'Connor, C. R.; Egle, T.; Kersell, H.; Oliver-Meseguer, J.; Salmeron, M. B.; Madix, R. J.; Sautet, P.; Friend, C. M. Dynamics of Surface Alloys: Rearrangement of Pd/Ag(111) Induced by CO and O_2. *J. Phys. Chem. C* **2019**, 123, 8312-8323.

(25) Aich, P.; Wei, H.; Basan, B.; Kropf, A. J.; Schweitzer, N. M.; Marshall, C. L.; Miller, J. T.; Meyer, R. Single-Atom Ally Pd-Ag Catalyst for Selective Hydrogenation of Acrolein. *J. Phys. Chem. C* **2015**, 119, 18140-18148.

(26) Davis, L. E.; MacDonald, N. C.; Palmberg, P. W.; Riach, G. E.; Weber, R. E. *Handbook of Auger Electron Spectroscopy*. Second ed.; Physical Electronics Industries, Inc.: Eden Prairie, Minnesota, **1776**.

(27) Hansen, W.; Bertolo, M.; Jacobi, K. Physisorption of CO on Ag(111): Investigation of the Monolayer and Multilaye Through HREELS, ARUPS, and TDS. *Surf. Sci.* **1991**, 253, 1-12.

(28) Guo, X.; Jr., J. T. Y., Dependence of Effective Desorption Kinetic Parameters on Surface Coverage and Adsorption Temperature: CO on Pd(111). *J. Chem. Phys.* **1989**, *90*, 6761-6766.

(29) Lee, G.; Plummer, E. W. Interaction of Hydrogen with the Ag(111) Surface. *Phys. Rev. B* **1995**, 51, 7250-7261.

(30) Lee, G.; Sprunger, P. T.; Okada, M.; Poker, D. B.; Zehner, D. M.; Plummer, E. W. Chemisorption of Hydrogen on the Ag(111) Surface. *J. Vac. Sci. and Tech. A* **1994**, 12, 2119-2123.

(31) Darby, M. T.; Sykes, E. C. H.; Michaelides, A.; Stamatakis, M. Carbon Monoxide Poisoning Resistance and Structural Stability of Single Atom Alloys. *Tops. Catal.* **2018**, 61, 428-438.

(32) Agrawal, V. K.; Trenary, M. An Infrared Study of NO Adsorption at Defect Sites on Pt(111). *Surf. Sci*. **1991**, 259, 116-128.

(33) Greeley, J.; Mavrikakis, M. Surface and subsurface hydrogen: Adsorption properties on transition metals and near-surface alloys. *J. Phys. Chem. B* **2005,** *109* 3460-3471.

(34) Tierney, H. L.; Baber, A. E.; Kitchin, J. R.; Sykes, E. C. H. Hydrogen Dissociation and Spillover on Individual Isolated Palladium Atoms. *Phys. Rev. Lett.* **2009,** *103* 246102.

(35) Baber, A. E.; Tierney, H. L.; Lawton, T. J.; Sykes, E. C. H. An Atomic-Scale View of Palladium Alloys and their Ability to Dissociate Molecular Hydrogen. *ChemCatChem* **2011,** *3* 607-614.

TOC Graphic